Radiation detector based on photovoltaic property of single-walled carbon nanotube

Rasun Kim

Department of Biomedical Engineering
(Life Sciences)

Graduate School of UNIST

Radiation detector based on photovoltaic property of single-walled carbon nanotube

A thesis/dissertation
submitted to the Graduate School of UNIST
in partial fulfillment of the
requirements for the degree of
Master of Science

Rasun Kim

11. 20. 2015
Approved by

Advisor
Chang Young Lee

Radiation detector based on photovoltaic property of single-walled carbon nanotube

Rasun Kim

This certifies that the thesis/dissertation of Rasun Kim is approved.

11. 20. 2015

signature

Advisor: Chang Young Lee

signature

Tae Yun Kwon

signature

Chaenyung Cha

Abstract

Single-walled carbon nanotube (SWNT) can be either metallic or semiconducting, and has been studied for developing electronic devices that outperforms existing ones. Among the many characteristics of carbon nanotube, photovoltaic property makes SWNT an effective component of a photodetector. Furthermore, the photodetector based on SWNT can be applied as an effective radiation detector when combined with a scintillator. P-type of semiconducting SWNT and N-type of Si were used to fabricate a photodetector as a component of a radiation detector. The detector responded to a broad range of wavelengths, especially from red to near infrared (NIR) range. Therefore, scintillator suitable to be combined with the SWNT photodetector also needs to emit in the same wavelength range. Eu and Sm doped $LuPO_4$, $ScPO_4$ and YPO_4 emit luminescence in the long wavelength range, and thus are expected to serve as an appropriate scintillator for a SWNT-based radiation detector.

Contents

List of figures

List of tables

Nomenclature

CNT	Carbon nanotube
SWNT	Single-walled carbon nanotube
DWNT	Double-walled carbon nanotube
MWNT	Multi-walled carbon nanotube
HiPco	High-pressure CO conversion
CVD	Chemical vapor deposition
NIR	Near infrared
SDS	Sodium dodecyl sulfate
wt %	weight percent
PR	Photoresist
Au	Gold
In	Indium
μCi	micro-Curie
Eu	Europium
Sm	Samarium
$LuPO_4$	Lutetium phosphate
$ScPO_4$	Scandium phosphate
YPO_4	Yttrium phosphate
BGO	Bismuth germanium oxide
PDMS	Polydimethylsiloxane

I. Introduction

After Chernobyl disaster in 1986 and Fukushima Daiichi nuclear disaster in 2011, many people were worried about radiation poisoning. Therefore, many nations started to investigate and develop the tools of radiation detection, shieling and absorption. Inventions in the field of radiation detection became the most important topic in research on radiation. Scintillation has also emerged as a key material to detect radiation after nuclear disasters. The one of the most attractive properties of a scintillator was that it produces luminescence when a high-energy photon crashes into scintillator. Scintillation luminescence could be identified visually and then can easily be changed with another technology.

Because a scintillator has a luminescence property under the radiation field, it is an essential ingredient of a radiation-detecting machine. Scintillators are used not only in radiation detectors, but are also more broadly applied in our everyday life, such as in X-ray machines, cameras, and similar devices that use high-energy photons. The most common usage of scintillators is in light sensors, such as a photomultiplier tube (PMT) (Figure 1). When the photon comes into the PMT, the initiation photons are amplified and this phenomenon makes the sensor much more sensitive. Additionally, when high-energy photons pass through a scintillator, the photons lose their energy and change to low-energy photons. The changed photons come into the PMT, crash into electrodes in the PMT and amplify during their passing through the PMT from the cathode to the anode. These pathways of photons make detection much more sensitive and safe. The high-energy photons are not directly detected by a radiation sensor; rather, the detected photons lose their energy before the sensing. That is the reason why their use is much safer than direct accept.

However, the original sensor type of the PMT needs sufficient volume for sensing and amplifying the equipment space. Necessary space of sensing and sensitive structure of a multiplier tube makes hard PMT as handy device and make expansive the detector. To enhance the strength and cover up the weakness of PMT, developing a simple, convenient, and portable radiation detector would be very helpful to ensure radiation safety.

Carbon nanotube (CNT), especially a single-walled carbon nanotube (SWNT), is expected to become one of the materials to make up for the shortages of the PMT. The photovoltaic properties of the SWNT are suitable for making electronic equipment. In addition, the sensor which is based on SWNT can be made in a small size, then, the total volume of a detector would be fabricated. The small volume makes the sensor application much broader. Therefore, in this research, the final goal is to make a radiation detector which would be based on the photovoltaic properties of SWNT. To get a high efficiency of the

sensor, SWNTs which were used as sensor material were separated by their chirality. The scintillator which emits the excitation wavelength for nanotube will be combined with the detector based on SWNT.

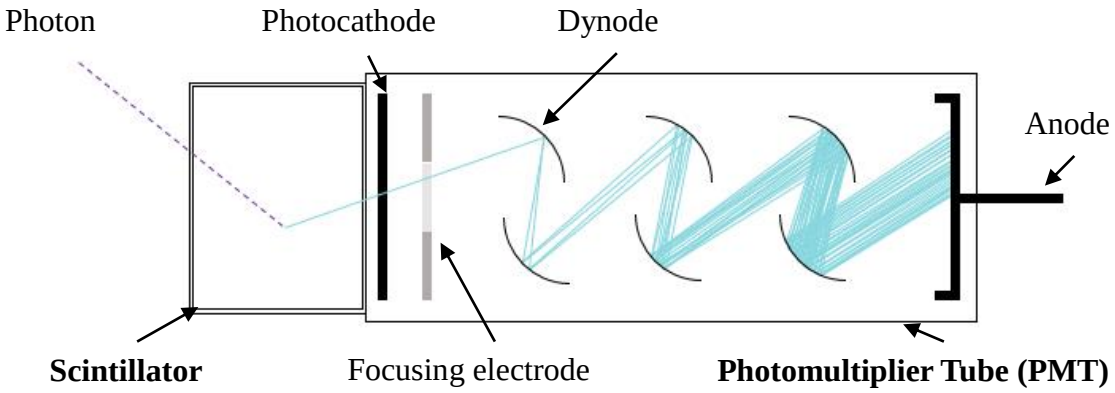

[Figure 1] The schematic design of photodetector which was Photomultiplier Tube (PMT) combined with scintillator.

II. Theoretical & Mathematical Development

2.1 Basic information of carbon nanotube

The discovery of carbon nanotube (CNT) was first reported by Sumio Iijima in *Nature*, 1991. [1] CNT is a kind of one-dimensional structure which was explained that a graphene sheet or graphene layers were rolled up.

CNT is few nanometers in diameter, but the length of CNT can reach several centimeters. Therefore, the surface-to-volume ratio of CNT is very high and it makes CNTs much more effective to react. CNTs have a high flexibility [21] and a low mass density [22]. In addition, carbon nanotubes have good electrical conductivity (Table 2) [33-40] and their thermal conductivity is higher than that of copper (see Table 1) [2]. Strong covalent bonds of carbon atoms of carbon nanotubes make CNTs chemically stable in the air condition. The bond strength of the carbon atoms is better than that of silicon.

Carbon nanotubes are divided into single-walled carbon nanotube (SWNT) and multi-walled carbon nanotube (MWNT) by the number of the layers.

2.1.1 Single-walled carbon nanotube

A single-walled carbon nanotube (SWNT) has one layer of graphene and its diameter range is 0.4 nm – 2 nm [25]. SWNT can have metal or semiconducting properties. In the case of the single-walled carbon nanotube, their properties are changed by the rolling direction of a carbon sheet or by their diameter. The layer of graphene is rolled with a paring number (n, m) (see Figure 2). A nanotube is called a zigzag nanotube when n=0 or m=0, and an armchair nanotube is a nanotube when n=m. If nanotubes was neither zigzag nor armchair, the nanotube was called chiral [26].

Semiconducting or metallic properties of nanotubes are determined by some coefficients of rolling vectors. Using tight-binding electronic structure calculations, many researchers predicted that the relationship between the coefficients (n and m) of the translational vector $C_h = n \bullet a_1 + m \bullet a_2$ determines the conducting properties. When 2n + m is an integer multiple of 3, a nanotube was shown to have metallic properties. Otherwise, nanotubes where 2n + m is not an integer multiple of 3, exhibit semiconducting properties [41].

2.1.2 Multi-walled carbon nanotube

A multi-walled carbon nanotube (MWNT) has multiple graphene layers that are rolled up. The distance between the layers of MWNTs is less than 0.34 nm and this distance is similar to that of graphite, 0.352 nm [23]. Since MWNTs have multiple layers, their diameter is bigger than that of SWNTs. Each layer of a MWNT has its own chirality, so it is difficult to define the overall chirality of a MWNT [25].

2.1.3 Properties of single-walled carbon nanotube for fabricating photodetector

Since single-walled carbon nanotubes have a wide range of band gaps [28], they can absorb a broad range of light. This characteristic makes SWNTs a proper material for fabricating photodetectors such as solar cells. One of the important properties of SWNTs for photodetector is that some kinds of SWNTs have semiconducting properties. To improve the efficiency of the electronic devices, usually, a P-N junction diode was made. Semiconducting properties of SWNTs make them appropriate ingredients for fabrication of P-N junction with other semiconductors [29].

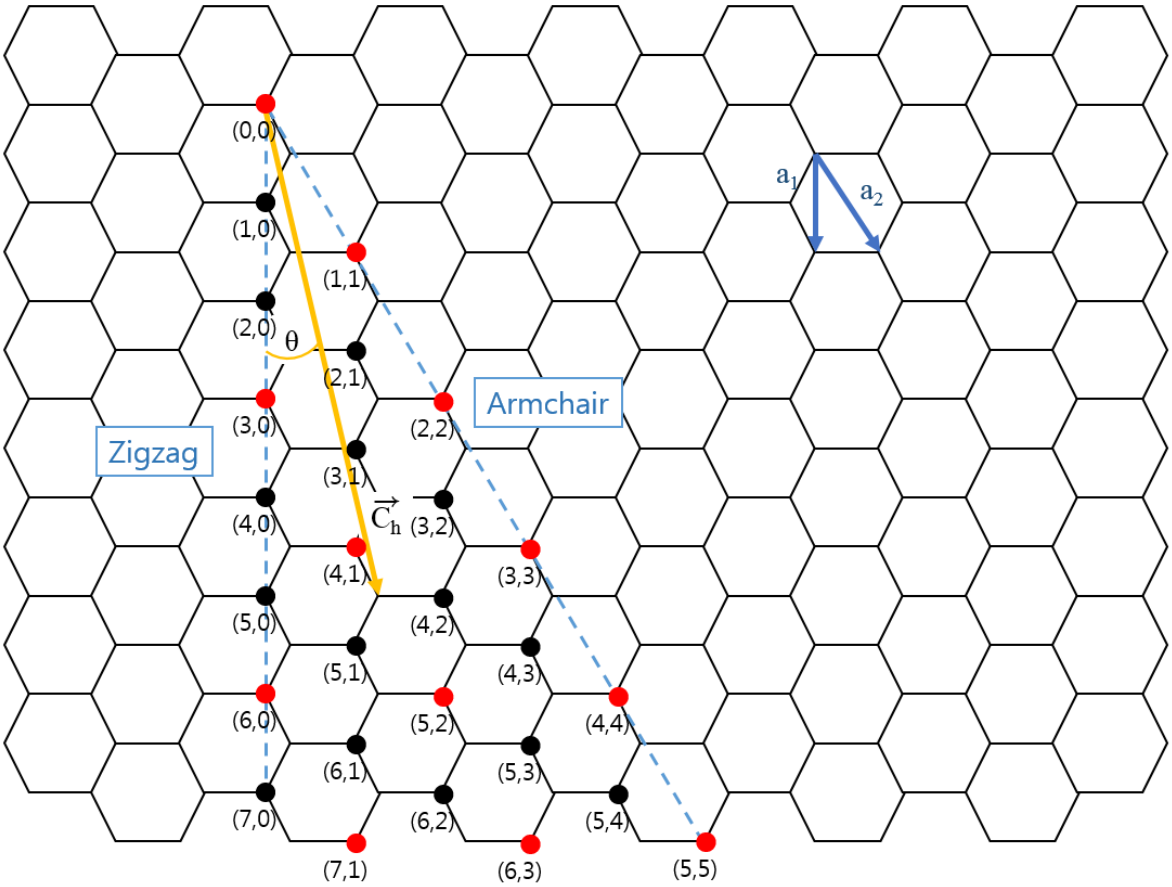

[Figure 2] Schematic of the graphene sheet. SWNT can be formed by wrapping the sheet along latties vector, n and m. zigzag, armchair, and chiral SWNT was formed. Red dots mean metal property and black dots mean semiconducting property.

[Table 1] Thermal conductivities of some carbon materials and metals [2, 14-18]

Material	**Thermal Conductivity at 25℃ (W/mK)**
Carbon Nanotube	2,000-6,000
Carbon Black	6-174
Graphite	100-400
Diamond	2,000
Copper	483
Silver	450
Gold	345
Aluminum	204

[Table 2] Electrical properties of CNT fibers with chemical treatments [33-40]

Type of CNTs	Fiber treatment	Diameter (μm)	Conductivity (S/cm)	Temperature (K)
MWNT		3	595.2	300
MWNT	Annealed in air 480 ℃	3	818.3	300
MWNT	Oxidized in 5 N HNO_3	3	969	300
MWNT	Arrays grown by water-assisted CVD	10-34	400-810	300
SWNT		50-500	1,400	90
SWNT	Annealed at >1000 ℃	60	382	300
SWNT	100 % H_2SO_4 (24 h, 100 ℃)	60	4,170	200
SWNT	Doped with HSO_3Cl	8-10	29,000 ± 3,000	60
SWNT	DNA dispersion, annealed at 1000 ℃	2-30	166.7	-
DWNT		10-200	5,000	-
DWNT	Oxidation (24 h, 350 ℃), immersion (37 % HCl, 48 h)	5-20	5,900	-

2.2 Scintillator

Scintillation material, a scintillator, is a material which has luminescence properties when exposed to radiation, high energy particles, and photons. The emitted light from the excited scintillator can be detected with a specific camera. Scintillator was first used as a ZnS screen in 1903. Afterwards, scintillators started to be used in various fields, including X-ray security, cameras, and medical equipment such as CT scanners.

Scintillators are typically categorized into organic and inorganic scintillators. Organic scintillators has immediately decay, but its scintillation efficiency is lower than that of am inorganic scintillator. Therefore, organic scintillators were used in α- and β-ray detectors. Inorganic scintillators have more sensitive scintillation properties than organic scintillators. Therefore, inorganic scintillators are usually used to detect γ-ray or X-ray. NaI(Tl), KI(Tl), and LiI(Eu) are classic inorganic scintillators. Sometimes, gaseous scintillators, such as ZnS(Ag) and Xe, were used.

When the rear earth ions are excited in room temperature, they emit a long wavelength of light (see Table 3) [30] Especially, Eu and Sm, rare earth elements, doped $LuPO_4$, $ScPO_4$ and YPO_4, scintillator was emitted in the 600-900 nm range (see Table 4) [20]. Additionally, undoped Hg_2Cl_2 has emission wavelength 720 nm.

[Table 3] Known rare earth solid state laser transitions (emission range: 600-900 nm) [30]

Wavelength (nm)	Ion	Transition
600	Pr^{3+}	$^3P_0 \rightarrow {}^3H_6$
610	Eu^{3+}	$^5D_0 \rightarrow {}^7F_2$
620	Er^{3+}	$^4G_{11/2} \rightarrow {}^4I_{11/2}$
620	Er^{3+}	$^2P_{3/2} \rightarrow {}^4F_{9/2}$
630	Pr^{3+}	$^3P_2 \rightarrow {}^3F_4$
640	Pr^{3+}	$^3P_0 \rightarrow {}^3F_2$
650	Sm^{3+}	$^4G_{5/2} \rightarrow {}^6H_{7/2}$
650	Tm^{3+}	$^1G_4 \rightarrow {}^3F_4$
670	Er^{3+}	$^4F_{9/2} \rightarrow {}^4I_{15/2}$
700	Pr^{3+}	$^3P_0 \rightarrow {}^3F_3$
700	Er^{3+}	$^2H_{9/2} \rightarrow {}^4I_{11/2}$
700	Sm^{2+}	$^5D_0 \rightarrow {}^7F_1$
720	Pr^{3+}	$^3P_0 \rightarrow {}^3F_4$
730	Nd^{3+}	$^2P_{3/2} \rightarrow {}^4F_{5/2}$
750	Ho^{3+}	$^5S_2 \rightarrow {}^5I_7$
800	Tm^{3+}	$^3H_4 \rightarrow {}^3H_6$
800	Tm^{3+}	$^1G_4 \rightarrow {}^3H_5$
850	Er^{3+}	$^4S_{3/2} \rightarrow 4I_{13/2}$
880	Pr^{3+}	$^3P_1 \rightarrow {}^1G_4$

[Table 4] Long wavelength Luminosities. The measured luminous intensity of the 600-900 nm emissions. [20]

Compound	Photon / MeV
$LuPO_4$: 20 % Eu	123,171
$ScPO_4$: ~1 % Eu	61,072
$ScPO_4$: 10 % Sm	44,302
YVO_4: Eu	35,728
$ScPO_4$: 3 % Sm	31,543
YPO_4: 2 % Sm	31,294
$GdTaO_4$: Tb	13,067
BaF_2: 10 % Eu	10,304
$LuPO_4$: 10 % Tb	9,316
$ScPO_4$: 10 % Pr	9,280
YPO_4:2% Tm	9,242
Hg_2Cl_2	7,886
LaF_3: 0.5% Pr	7,824
ZnS:Ag	7,057
$LuTaO_4$:Tb	6,539
TiO2	4,399
$BaNb_2O_6$ * $SrNb_2O_6$	4,293
CdS	4,029
$Bi_2Al_4O_9$	3,856
SrI_2	3,786
ZnO	3,216
Hg_2Br_2	3,036
CsI	2,690
YPO_4 5% Nd	2,571
Eu_2O_3	2,497
$Bi_2Al_4O_9$: 0.5% Ce	2,296
BaF_2 8 4% Ho	1,806
$Lu_3Ai_5O_{12}$: Ce	1,514
$A1_2O_3$	1,389
BaF_2: 10 % Er	1,133
ZnO: 0.6% In	1,025
Bi_4Ge_3O12	1,011
CdF_2: 10 % Tb	994
$LuPO_4$: 40 % Pr	939
ErF_3	932

III. Experimental Method & Materials

3.1 Carbon nanotube solution

One of the effective methods to use carbon nanotubes is using them in separated by their chirality. SWNTs have semiconducting or metallic properties. Semiconducting properties of SWNTs are much more suitable in terms of SWNTs use in electronic devices. That's the why separated nanotube solution I need in this research. To classify SWNTs, they must first be dissolved in a solvent before separation. The procedure was as follows:

1. 10 mg SWNTs (HiPco) were dissolved in 100ml 2 weight % sodium dodecyl Sulfate (SDS) solution.
2. The nanotube solution was sonicated using Tip Sonicator (VCX130, SONICS & MATERIALS INC.) for 5 hours. The power of the sonication was 30 watt.
3. The solution which from 2 was centrifuged at 40,000 RPM for 3 hours using Ultracentrifuge (Optima L-100 XP, BECKMAN COULTER).
4. Only 70-80 % of upper solution after centrifugation was used.

The procedure of making a carbon nanotube solution could be explained with 4 steps. Each step looks simple, but it makes to be sensitive a reputable nanotube solution. The first thing to be concerned with is temperature. The sonication step is an exothermic process. During the sonication step, control of the temperature of the nanotube solution is crucial. During sonication for several hours, without temperature control, the temperature of nanotube solution increases and causes assembling of carbon nanotubes into bundles. The bundles of SWNTs interrupt the interaction between SWNTs and SDS molecules. Therefore, the icing step during the sonication is very important [3,5]. According to Shi et al., appropriate temperature of the SDS solution to dissolve a nanotube is 24 ℃ [4]. Nanotube solution of 24 ℃ has a higher absorbance value than the solution of 30 ℃. However, a lower temperature is also not good for the SDS solution. When the temperature of the SDS solution is lower than 15 ℃, the affinity between SDS and carbon nanotube is changed. Surfactants are much more familiar with large-diameter nanotubes in the lower temperature condition. In cold temperature, all kinds of carbon nanotubes might not resolve in the solution. Just like during the sonication process, the temperature in

the centrifuge is also important. Therefore, it is important to be careful when controlling the temperature of the solution.

3.2 Separation of Carbon nanotube by chirality

Carbon nanotubes were shown to have various properties depending on their chirality [6]. In the pristine nanotube solution, all types of SWNTs were mixed without separation. For the effective usage of SWNTs, they would have to be separated by their properties. In this experiment, the method suggested by Liu's group was used to separate HiPco nanotube. [3] The original process was added to the method reported by Liu's group. The sequence was as follows:

1. 2ml sephacryl gel (S-200) was filled in the column of 10ml syringe column.
2. 2 wt % SDS solution was loaded in the column, for stabilizing sephacryl gel with the SDS solution.
3. After stabilizing sephacryl gel, the SWNT solution was allowed to pass through the gel.
4. When all the SWNT solution have passed through the gel, the gel was washed with 2 wt % SDS solution (the washing step).
5. If the color of the gel was still black after the washing step, the column was dumped and steps 1-4 steps were repeated.
6. When the color of the gel changed (ex, blue, violet, or green) after the washing step, 5 ml of 5 wt % SDS solution were loaded into the column. The results were collected separately (the elution step).
7. Step s1-4 and 6 were repeated with the result solution of step 3.

If color of the gel did not change after the SWNT solution passed, or if the color of the resulting solution in step 3 has changed to yellow, the experimental process was stopped and the absorbance of the eluted solutions and SWNT solution passing through the gel were checked.

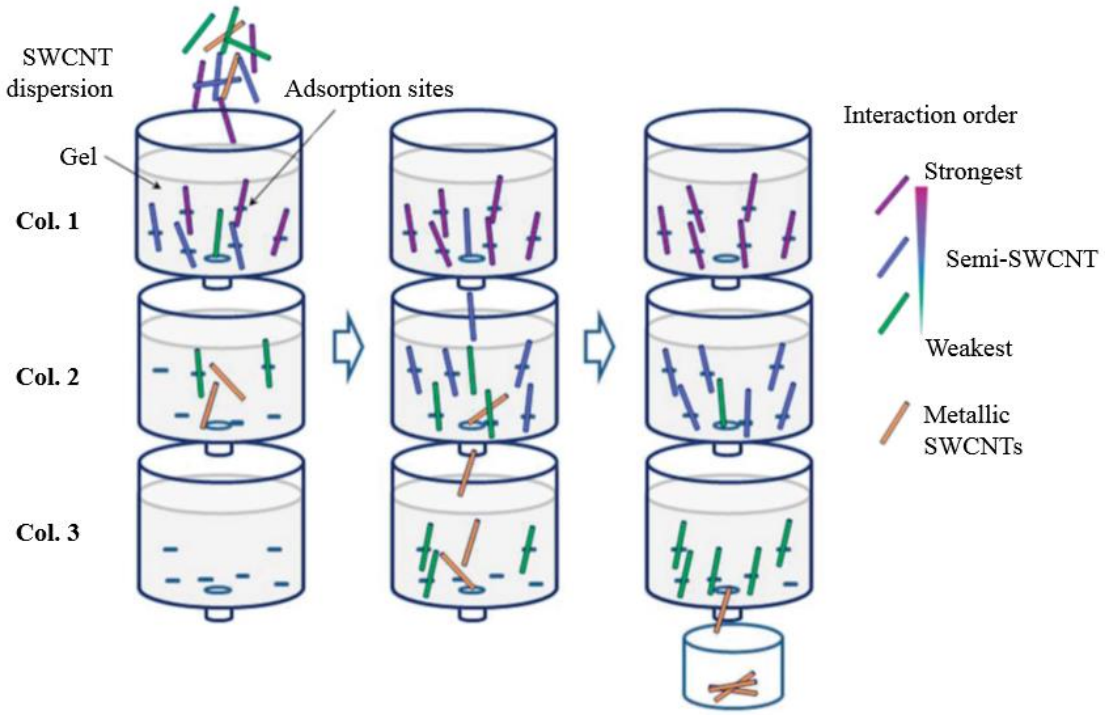

[Figure 3] Schematic diagram of chirality separation of SWNTs using single-surfactant multicolumn gel chromatography. [3]

Because amorphous carbons have the highest affinity to sephacryl gel, amorphous carbons were attached to the gel in first. Step 5 was meant for filtering amorphous carbon. Afterwards, each type of SWNT was attached to sephacryl gel in sequence. SWNTs with semiconducting properties have a higher affinity to gel than SWNTs with metallic properties. As the final result, semiconducting SWNTs were separated in order and then metallic SWNT finally remained in the nanotube solution (Figure 3) [3].

3.3 Nanotube film making

The surfactant, SDS, is the key material that lets the carbon nanotube get dispensed in the solution; however, it is an obstacle when the SWNT film is made. Carbon nanotube is good to be used as a part of electronic device. Used nanotube in the solution as an ingredient of electronic device, the surfactant, SDS, would be impurity, so it has to be removed and it is better to use getting pure SWNT to be applied to another device. For gathering the pure SWNT, filtration is a widely used method [7]. SWNT film which was fabricated by membrane filtration is much more effective and dense than that fabricated by other methods, such as the dry method. In this experiment, regarding the next procedure, we used mixed cellulose ester (MCE) membrane (Millipore, pore size 25 nm). The sequence was as follows:

1. Semiconducting SWNT solution was diluted 20-50 times which was extracted by the gel separation method.
2. The MCE membrane was set on the filtering flask and fritted glass support. The glass column was put on the membrane and the support and column were gripped with an aluminum clamp.
3. 1 ml of the solution from step 1 was loaded and vacuum filtration was done.
4. After SWNT solution passed through the MCE membrane, sufficient amount of DI water was loaded for washing (the washing step).

Dilution ratio was controlled by the eluted SWNT solution. Mostly, the color of the solution changed so that to become pale after dilution. Depending the concentration of the diluted SWNT solution, the volume of the loaded SWNT solution in the column can be adjusted. In the case of pale concentration, ca.1 ml of solution is sufficient to make film. If the volume of SWNT solution is less than 1 ml, the

density of the film would not be equal on the surface of MCE membrane. Due to the affinity with glass and water, the edge of the film would be much denser than the center of the film.

3.4 SWNT Membrane Transfer

SWNT film can be used in the gray, but it is usually transferred to other substrate, such as glass, silicon or indium tin oxide (ITO). [8] The reason that used MCE membrane to make SWNT film was for transfer step of SWNT film. MCE membrane could be melt with acetone. That's the why MCE membrane was preferred to transfer. The goal of this research was making a sensor based on carbon nanotube. Depending on the design of the sensor, substrate would be changed. To make electrode interdigitated sensor, silicon oxide wafer is need to fabricate sensor. Or silicon wafer is needed to make a sensor which let the electrons pass through substrate from electrodes. If fabricate interdigitated sensor, producing SWNT film on wafer by chemical vapor deposition (CVD) method is much easy to control than transferring SWNT film. However CVD method is fitted to grow carbon nanotube on silicon oxide substrate, because of oxidation during high temperature treatment. In this experiment, SWNT film have to be transferred on silicon substrate without oxidation of substrate. Therefore SWNT film would be transferred on n-type silicon wafer with following sequence.

1. Cut n-type silicon wafer as MCE membrane or smaller size after remove dust on the wafer.
2. Remove the natural oxidation layer on Si wafer soaking in buffered oxide etchant (BOE), also known as buffered hydrogen fluoride (Buffered HF), for several seconds.
3. Drip a drop of ethanol on Si substrate and overlap with substrate and SWNT film on the MCE membrane.
4. Bake SWNT film combined to substrate from step 3 on oven at 90 ℃ for 1 hour. Supply moisture enough during baking.
5. After bake, soak SWNT film combined to substrate into acetone to melting MCE membrane.

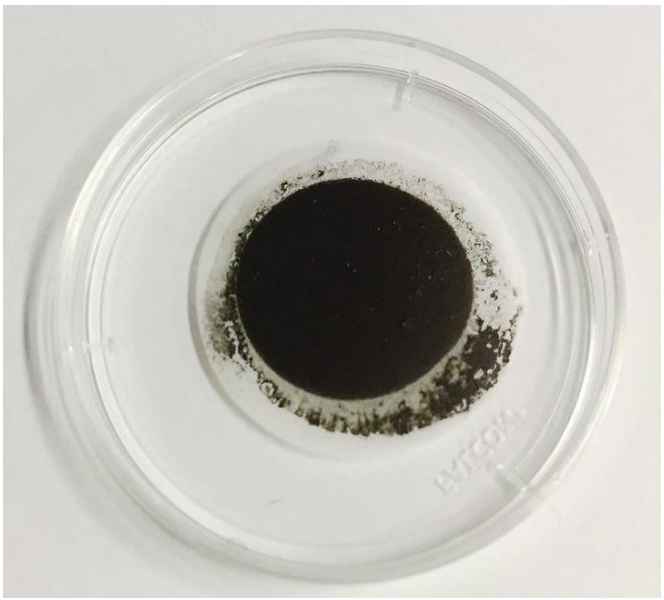

[Figure 4] Vacuum filtrated SWNT film (non-diluted SWNT solution) on MCE membrane.

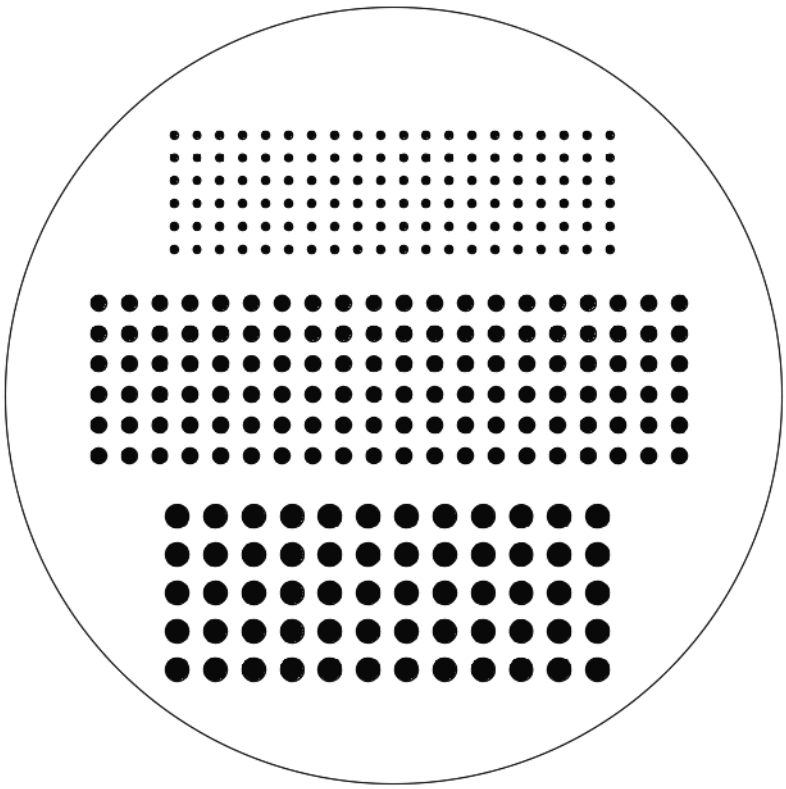

[Figure 5] The pattern mask design for window of Photodetector. The white part was cleared and light pass through clear part. If used positive photoresist

3.5 Mask pattern

Film mask plays an important role in fabricating electrodes on a sensor. Gold electrode would be deposited on the top side of a photodetector. The design of mask pattern was decided by the character of the photodetector. Since the light has to be come in to the photodetector, a gold electrode has a circle shape like a window to take light. The amount of incoming light affects the work of the sensor. Therefore, it is important to consider window size. Finally, the windows have 1 mm, 2 mm, and 3 mm of diameter (see Figure 5).

3.6 Sensor fabrication

Electrode is very important part to electronic device to link wire and be applied. In this experiment, the sensor design was referred solar cells form Wang et al. [9] Solar cell is most typical type of photodetector. Sunlight stimulated nanotube and voltage was generated under light exposure. Because photovoltaic property of nanotube was the representative for producing photodetector, the part of gathering the light is needed. Therefore, the circle shapes of window patterns were designed on photomask. Electrodes would be fabricated with photolithography technique. Moreover, to improve detecting the light, pristine SWNT (p-type) and n-type of Si wafer were used to make P-N junction part of sensor. The following sequence is:

1. Dust or impurities on the n-type Si wafer were removed and photoresist (PR; AZ5014E, positive PR) was poured on the wafer.
2. Si wafer was spincoated at 4000 RPM, for 40 sec.
3. Si wafer was baked on a hotplate at 105 ℃, for 1 min 30 sec (soft baking)
4. The photomask was aligned and the Si wafer coated by PR on the stage of UV exposure was fixed.
5. Exposure UV light on Si wafer through photomask. The power of UV was 100W.
6. PR on Si wafer dipped developer. Afterwards, the remaining developer on Si wafer was washed by DI water.
7. The photoresist pattern was checked and gold was deposited on the pattern (Cr/Au, 2/80 nm).
8. Au on PR was lifted off with soaking acetone. If PR and unnecessary Au part doesn't remove well, Si wafer was sonicated for a few seconds in bath sonication.

The bottom of the wafer was scratched and indium was attached to the bottom of the wafer (gold electrode was placed on the top side of sensor)

(a)

(b)

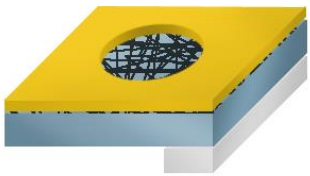

(c)

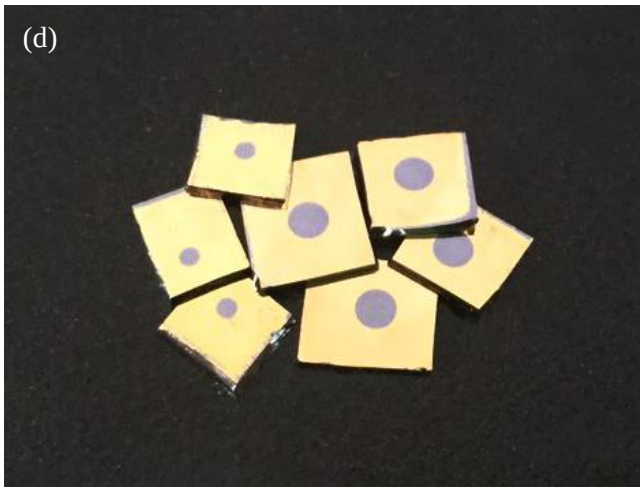

[Figure 6] Schematic and complete product of photodetector based on SWNT. (a) Components of photodetector (b) perspective (c) side view, and (d) photodetector which have 1 mm and 2 mm window.

3.7 Photovoltaic property and radiation affection of voltage

One of the properties of carbon nanotube is absorbing light and observed photovoltaic property, especially in the near infrared range [10], meaning that a photodetector based on carbon nanotube can effectively work near IR. Therefore, the goal of this research was to find an effective scintillator which can emit wavelength, excite carbon nanotube, and fabricate a radiation sensor combined a suitable scintillator.

To finding a suitable scintillator, the information of SWNTs which were used to make the detector is needed, especially, the absorbance information by each wavelength. To measure absorbance by wavelength, the experiment to check photovoltaic property was carried out with NanoLog, a series of spectrofloromets (HORIBA). Xenon lamp which was built in NanoLog can emit the whole range of light, UV to NIR. The photodetector on stage of NanoLog and exposure sensor by the light from xenon lamp, 400 nm to 1150 nm. Voltage of the detector based on SWNTs was measured with the changed wavelength. The voltage change was observed with Digit Multimeter (34410A, Agilent).

3.8 Voltage affected by radiation

The final goal of this research is fabricating a radiation detector based on separated single-walled carbon nanotubes. Carbon nanotube has a good conductivity and is also affected by radiation itself [11, 12]. How much a sensor was affected by radiation is very important to consider. If voltage change was bigger than changed by photovoltaic, the result of photovoltaic could not be taken clear. Therefore, the voltage change by radiation was also measured in this experiment.

Voltage of the detector which was based on carbon nanotube was measured as to whether the radiation source was accessed or not. Radiation source was Cs-137, 1 μCi. It was close to 1 cm at the front of the SWNT sensor.

3.9 Combined photodetector with bismuth germanium oxide

Bismuth germanium oxide (BGO) is one of widely used scintillation materials in the world. When exposed to γ-ray, BGO emits luminescence in 480 nm. Because BGO powder is cost-effective and accessible, it was tested in combination with the photodetector as a scintillation part of the radiation

detector based on the nanotube. Combining BGO powder and the photodetector, two methods were tried in this research.

The first method was making BGO sheet with polydimethylsiloxane (PDMS). BGO was not mixed with silicon polymer, so it was trapped in PDMS forming a thin BGO layer at the bottom. Silicon elastomer (Sylgard 184) and silicon elastomer base (Sylgard 184) in the ratio one to ten were blended. BGO power was added and the mixture was missed with a homogenizer. After stabilizing the mixture in vacuum, it was baked in dry oven at 60 ℃ for 4 hours.

The second method was putting BGO powder directly on the detector with the mixture of the solution. Pure acetone was dried fast in room temperature and it did not affect to properties of BGO powder. The mixture of BGO powder and acetone was sonicated and the mixture was dropped on the photodetector. After drying, BGO powder remained on the detector.

IV. Result

The fabricated photodetector based on carbon nanotubes has a simple structure (see Figure 6). This type of photodetector is based on the structure of solar cell reported by Wang et al. [3]. The sensor used the theory of P-N junction, the intermediate between n-type of silicon wafer, and p-type of SWNTs. Excitation light came into the window pattern and excited the SWNT film on the sensor. Then, voltage occurred between the p-type carbon nanotube and the n-type silicon wafer, P-N junction [10]. The voltage change was observed when connecting gold and indium electrode by Digit Multimeter (34410A, Agilent).

4.1 Separated HiPco nanotube by gel separation

Pristine HiPco nanotube solution and separated HiPco nanotube solution (column 5) of excitation and emission wavelength were observed by NanoLog, because different types of SWNTs were excited by different wavelengths and emitted different wavelengths. In Figures 7-8, SWNTs were exited, between 450 nm and 800 nm, and emission wavelength was measured in 850 nm 1600nm. In the case of pristine SWNT, many different types of SWNTs were mixed in the solution. Otherwise, in the separated SWNT solution (column 5), many peaks were removed and the remaining enriched SWNTs were excited by long wavelength. Especially the SWNT solution in column 5 was enriched (10,2) (9,4), and (11,3) (see Figure 8) .This separated solution (column 5) was used to fabricate the photodetector based on SWNTs.

4.2 Transferred HiPco nanotube film on n-type Si wafer

Transferred SWNT film can be checked on Scanning Electron Microscope (SEM; S-4800, Hitachi High-Technologies). In Figures 9 and 10, carbon nanotubes were placed in the window of the photodetector. Because the film was formed by vacuum filtration, SWNTs formed a random network on the membrane. The thickness of SWNT film can be controlled by concentration and the amount of separated SWNTs solution which was used to make SWNT film. In this research, the detector was fabricated with Si wafer which was nanotube transferred by checking under SEM.

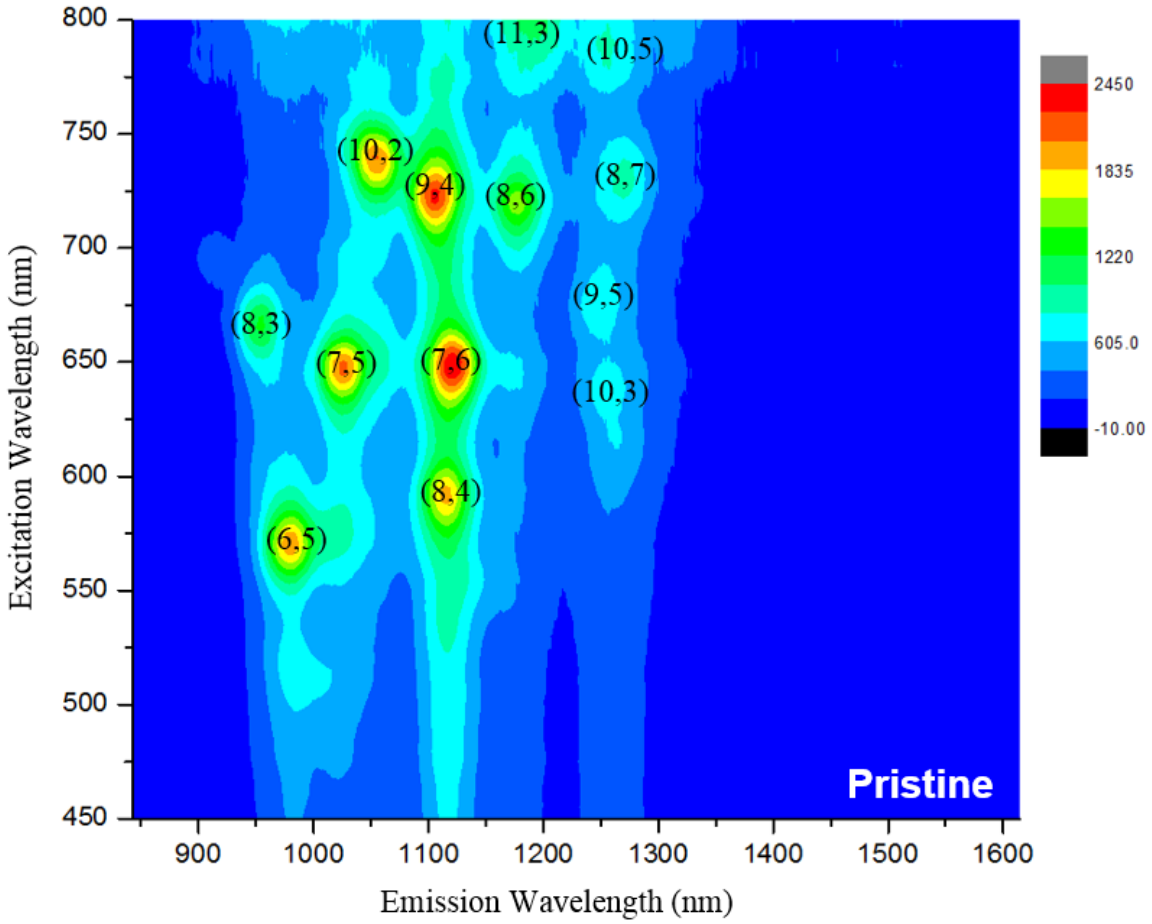

[Figure 7] Photoluminescence contour maps of pristine HiPco nanotube (n, m) fractions.

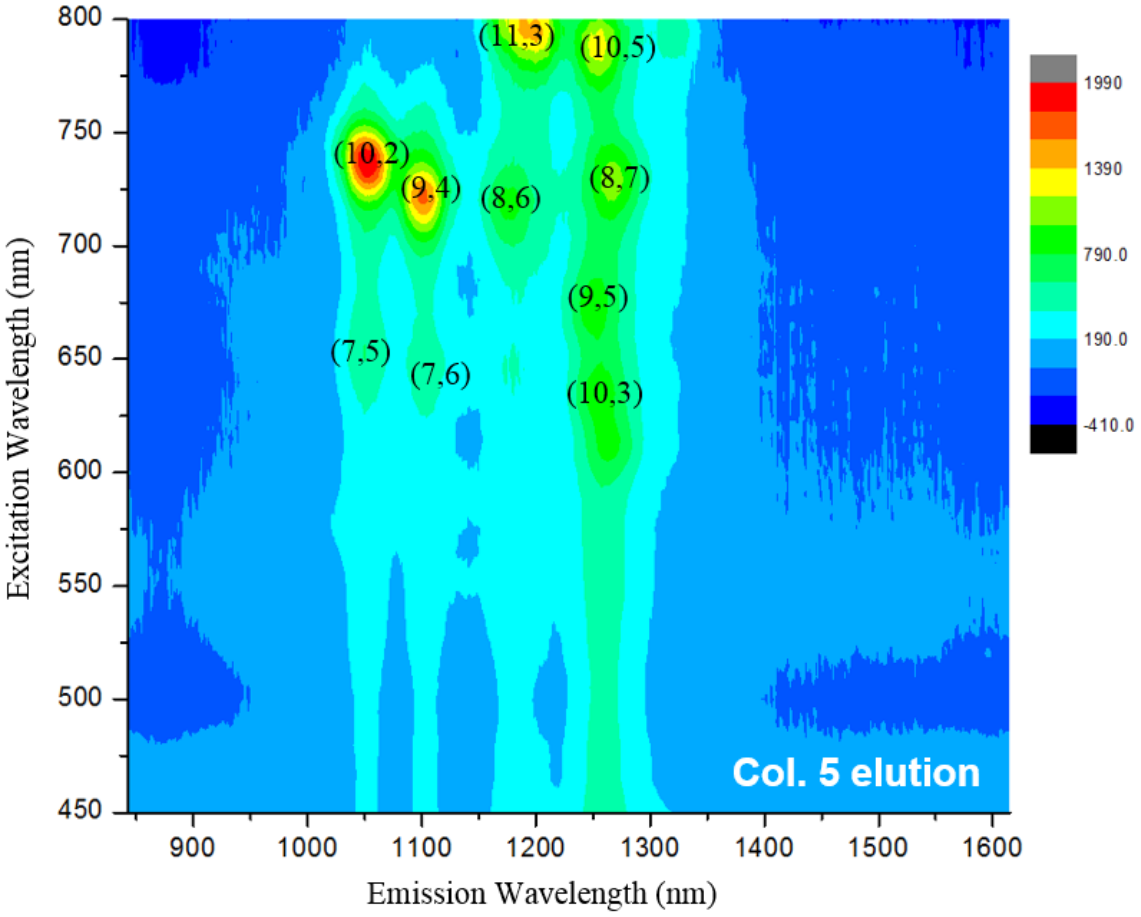

[Figure 8] Photoluminescence contour maps of 5th column elution with sephacryl gel separation HiPco nanotube (n, m) fractions.

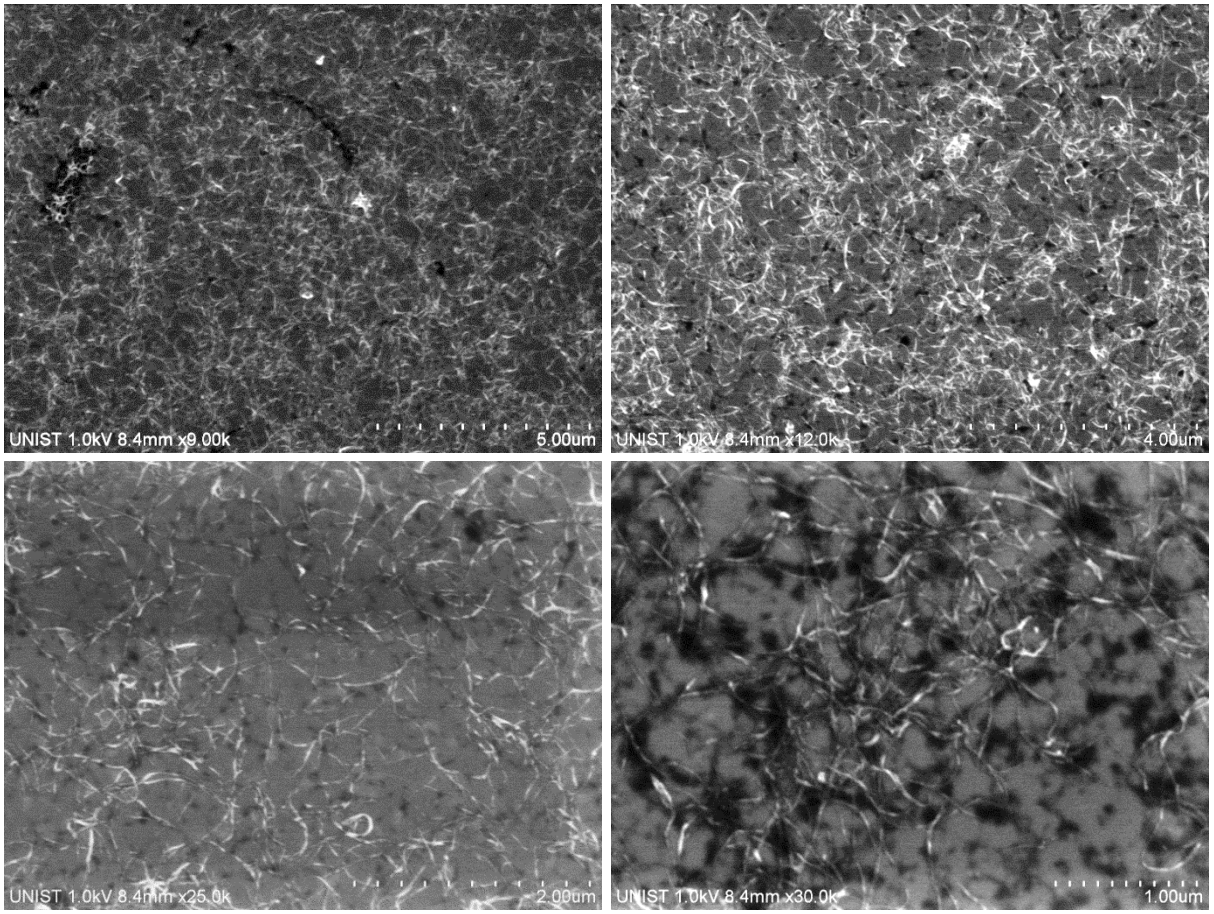

[Figure 9] SEM top view of transferred random-network SWNT film on n-type of Si wafer.

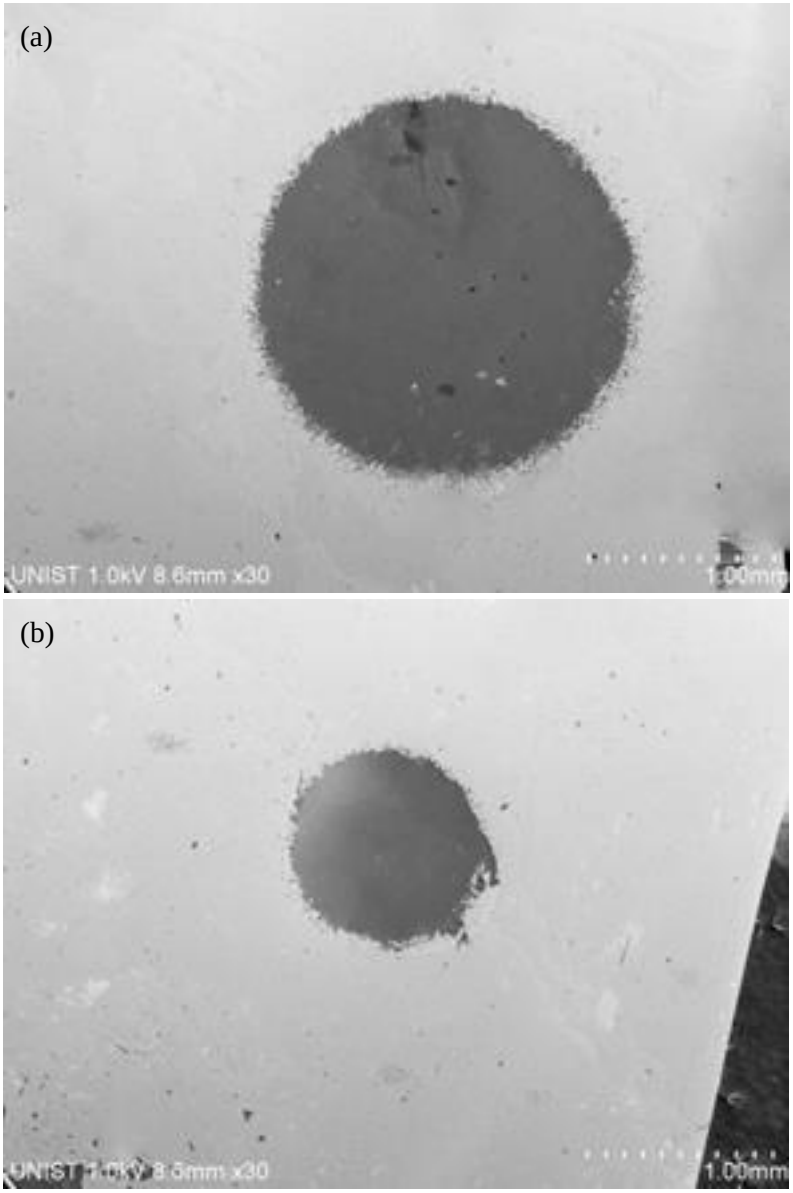

[Figure 10] SEM images of photodetector which have (a) 2 mm and (1) 1 mm window.

4.3 Photovoltaic property of photodetector based on SWNTs

Photovoltaic property of the SWNT photodetector was measured with haloid lamp (AmScope, 150W). Voltage occurred when the haloid lamp was on. Right after the lamp was turned on, voltage rapidly increased. Also, when the lamp was turned off, voltage dramatically decreased and went back to the original value (see Figure 11a).

Not only was the light as a factor to evoke voltage, but also the intensity of the light affected the voltage change of the detector. In the Figure 11b, the voltage change can be checked depending on the light intensity. The value of the voltage increased with the increase of the light intensity.

However, after some point of light intensity, the voltage remained at the regular value. This phenomenon was observed in other sensors which had different thickness of the carbon nanotube film or difference sizes of the window. The thicker SWNT film or the larger size of window, the larger change of voltage occurred.

4.4 Photovoltaic property of SWNT photodetector by wavelength

Since single-walled carbon nanotubes absorb specific wavelength, the photodetector based on SWNTs showed a different efficiency in each wavelength. The change of voltage by Nanolog in various wavelengths is shown in Figure 12a. The amount by which voltage changed seemed to have remained at a regular value. However, this did not apply to the power in each wavelength. Therefore, the real efficiency of the photodetector could be examined with dividing and normalizing the observed voltage changed by power in each wavelength (see Figure 12b). Furthermore, the real efficiency of the photodetector was calculated (see Figure 12c). Since a shorter wavelength has a larger power, the shape of the graph changed from the observed voltage changed result. According to the calculations, the ranges around 800 nm, 850 nm, 1150 nm, and much longer were more effective than other ranges.

(a)

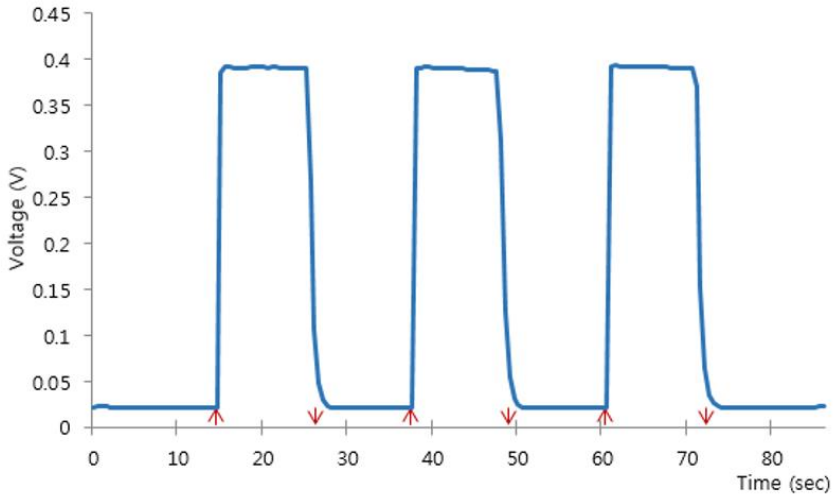

(b)

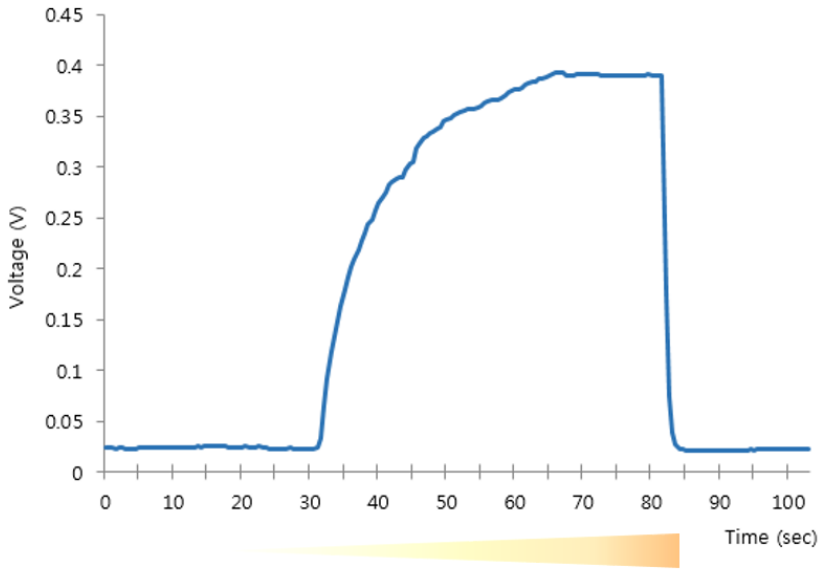

[Figure 11] Photovoltaic property of photodetector based on SWNT. (a) Voltage occur during lamp on/off (upside red arrows mean turn on, downside red arrows mean turn off) (b) voltage occur during lamp intensity getting increased.

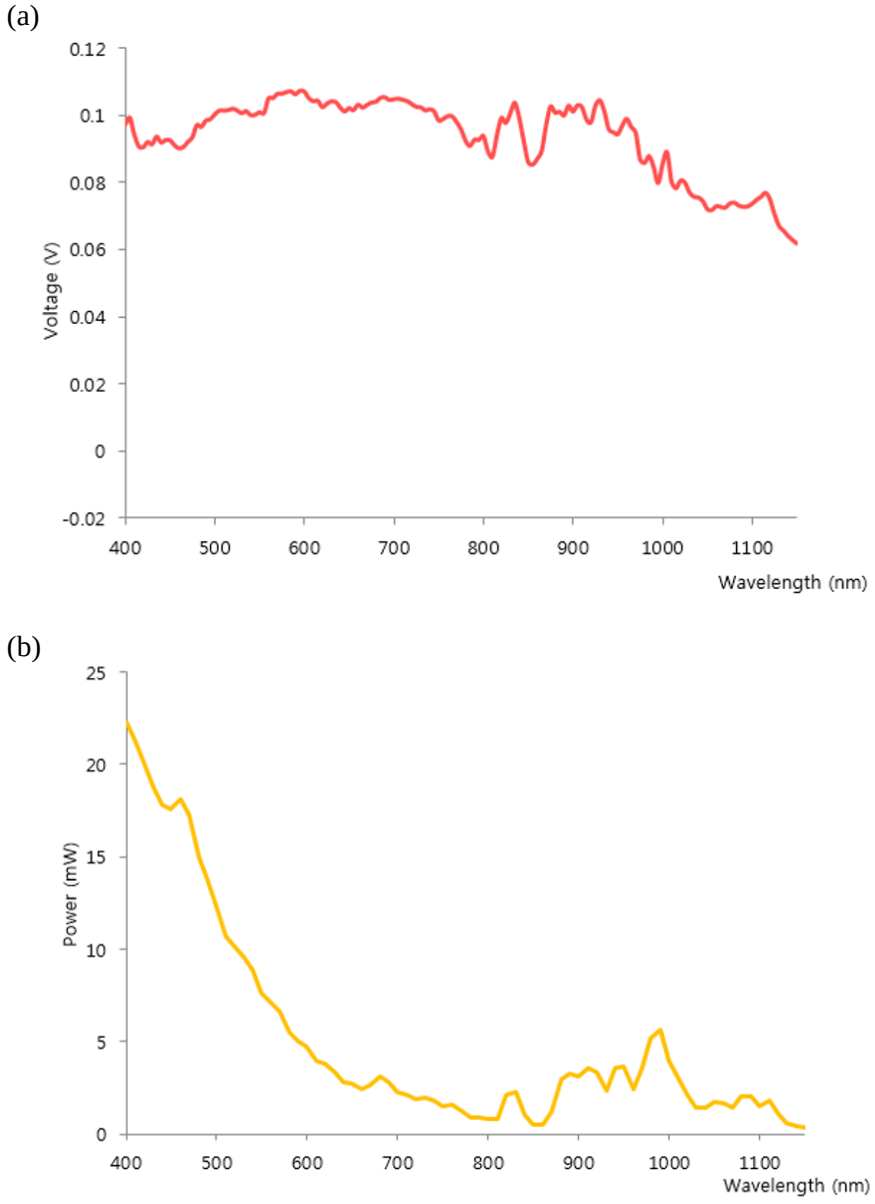

[Figure 12] Photovoltaic property of photodetector based on SWNT in each wavelength. (a) Measured voltage in each wavelength, (b) light intensity of xenon lamp in NanoLog, and (c) calculated efficient of photovoltaic property dividing voltage value by intensity of lamp. (Voltage/power)

(c)

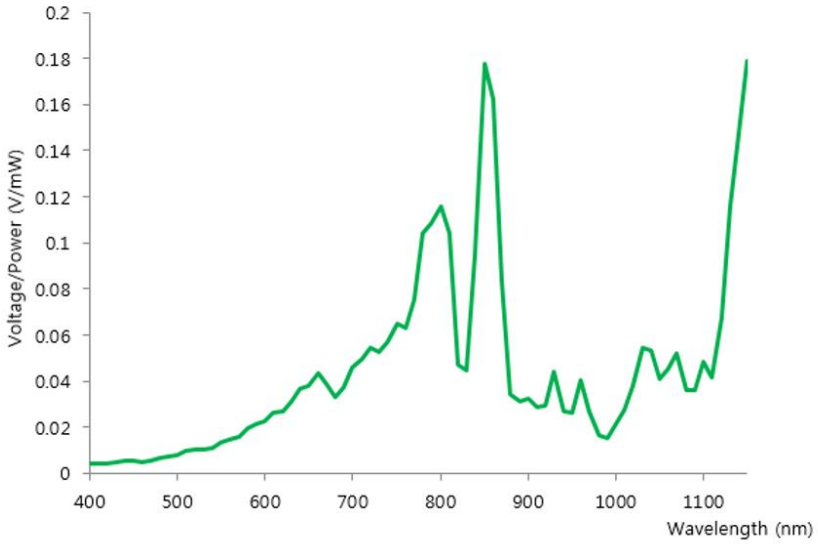

[Figure 12] (Continued)

4.5 The effect from weak gamma-ray radiation source

The final goal of this research is fabricating a radiation detector with SWNTs. However, since the SWNT affected by radiation [11, 12], the amount of radiation effect has to be measured. When the detector is exposed to radiation, gamma-ray from cesium, the voltage decreases (see Figure 13). As compared to voltage in the pristine state, almost 60% was off when the radiation source came closer. When the radiation source was far away from the sensor, decreased voltage returned to the original value. However, voltage decreased, the absolute changed value by radiation was much smaller than increased by photovoltaic property. This value can be ignored.

4.6 Effectiveness of bismuth germanium oxide in SWNT radiation sensor

Combined with the photodetector based on SWNT, BGO was tested for its scintillation efficiency in a radiation detector. The voltage change was observed with Digit Multimeter. Voltage did not increase during radiation source closer; rather, it decreased in both methods: BGO sheet or BGO powder (see Figure 14).

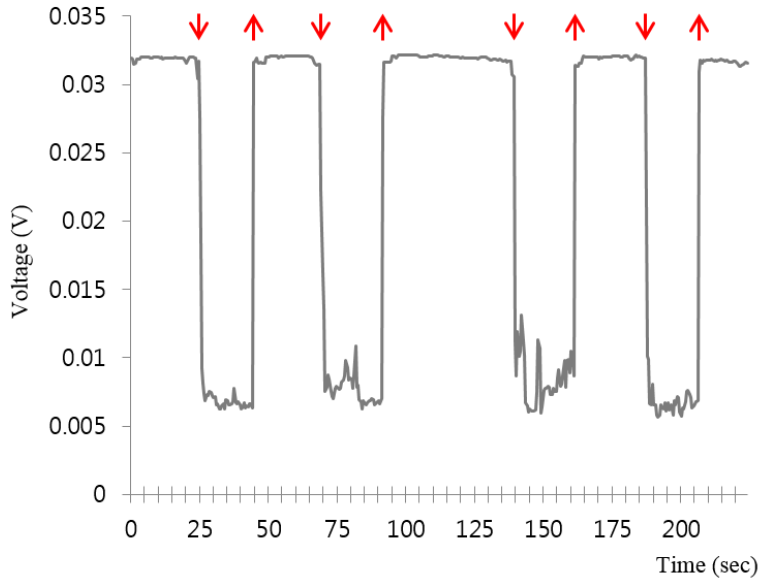

[Figure 13] voltage decreased when the radiation source approached to photodetector based on SWNT. (Downside red arrows mean radiation source came closer, upside red arrows mean go far away)

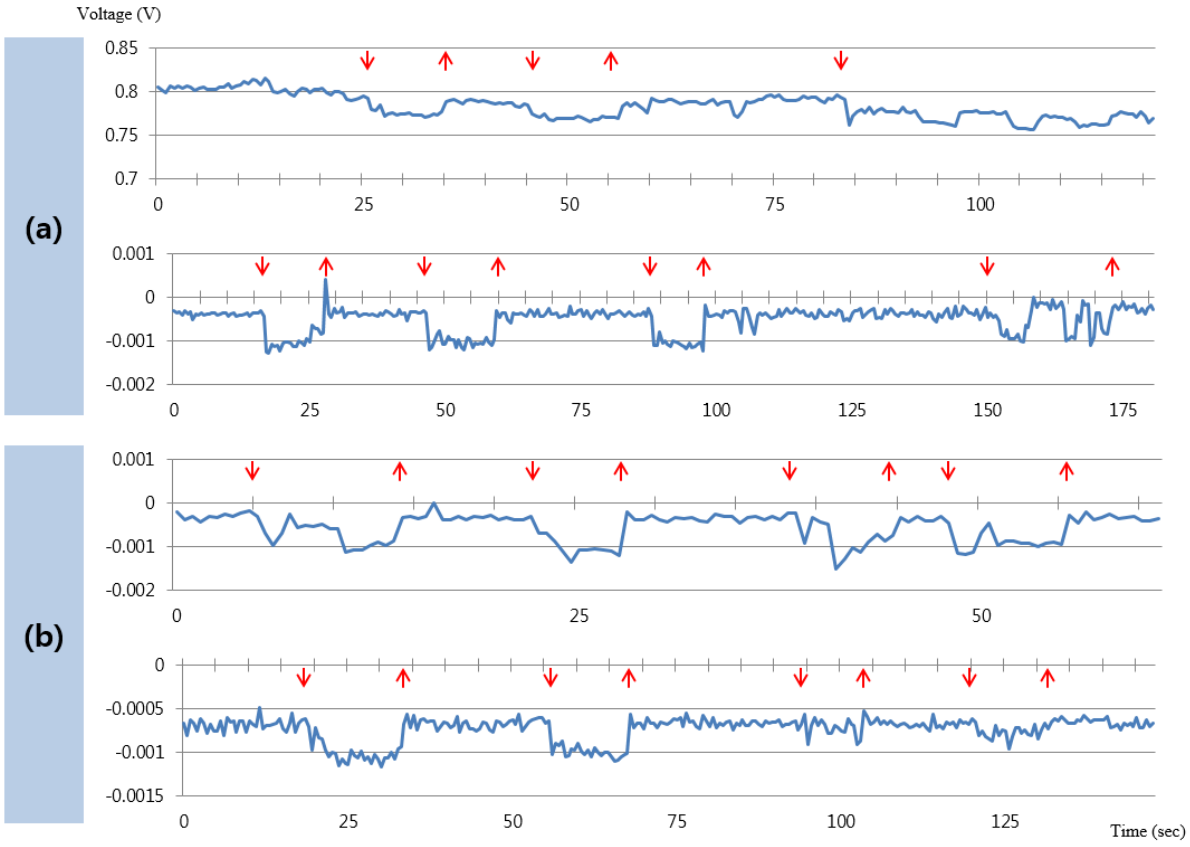

[Figure 14] Voltage variation of SWNT detector combined with BGO powder. (a) BGO and PDMS sheet, (b) BGO powder after drying acetone droplet. (Red arrows mean the radiation source come closer (downside) or go far away (upside))

V. Discussion

Figure 12c shows the property of the photodetectors based on SWNTs. Since photodetectors were fabricated based on SWNTs, the property of detectors was the same as those of carbon nanotubes. The sensor effectively worked at a long wavelength, near IR. This is the same as the property of nanotube that SWNTs were excited by long wavelength and emitted fluorescence [13]. In Figure 12c, the voltage change was great in 800 nm, 850 nm, 1150 nm, and longer. Compared to the excitation wavelength of separated SWNTs (see Figure 8), the excitation range of separated solution and the effective voltage changes of the detector seemed similar. It seems to be related to the kind of SWNTs chirality.

As shown in Figure 8, the separated SWNTs solution was enriched with (10,2) (9,4), and (11,3) chirality. In particular, (11,3) was exited at 800 nm and emitted 1200 nm wavelength. 800 nm of wavelength was the range of the shown grate efficient of the detector. From these results, it can be hypothesized that the effective work wavelength of SWNT detector can be affected the kinds of SWNTs used. For example, (6,4) nanotube was excited 600 nm and emitted 850 nm. (12,1) nanotube was excited 800 nm and emitted 1160 nm [3]. Assuming that the hypothesis that the efficiency of SWNT detector would depend on the chirality of used SWNT was correct, the excitation range of the photodetector can be controlled by separation of SWNTs.

This hypothesis is very important to the fabricated radiation detector combined with a scintillator. Radiation detector has a structure combined with a photodetector and a scintillator as the excitation light source. That means that the kind of scintillator can affect to the work of the radiation detector. Each scintillator has its specific emission peak. As a result, the emission wavelength from the excited scintillator lets the detector work. If the hypothesis is correct, the photodetector is expected to show the highest efficiency when the emission peak of the scintillator and the excitation range of the detector are the same.

If bismuth germanium oxide (BGO) was used as a scintillator in the radiation detector, radiation detector would not work well. The emission peak of BGO was 480 nm and the efficient of photodetector based on SWNTs was 1,011 photon/MeV at 480 nm. This value was 35.6% of CsI intensity [19, 20]. Moreover, the luminous intensity of BGO was not strong. These properties of BGO interrupt the detector working as an efficient radiation detector (Figure 14). To improve the radiation detector, other scintillators which emit longer wavelength are needed for the fabrication of a radiation sensor combined with SWNT sensor. Replacing with other scintillators which emit a stronger luminescence can be a method to improve the radiation detector.

Beside the change the scintillator, the detector can be improved by other factors. The window size of the detector can affect the thickness of the SWNT film which is the main component of the detector; it can also affect the amount of voltage change. The larger the window or the thicker the SWNT film, the more sensitively the detector works.

Further research should aim to fabricate an efficient radiation detector taking into consideration recommendation for improvement suggested in this paper, including separating each chirality of SWNT, a scintillator matching with each chirality of SWNT, large window size, and thickness of the nanotube film. With these factors, an improved radiation detector based on single-walled carbon nanotubes can be fabricated. Therefore, the final goal, fabrication radiation detector combined with scintillator and photodetector based on SWNTs, will be applied with various improvements and the efficient radiation detector in each condition will be found.

VI. Conclusion

In this research, the ultimate goal was to create a radiation detector that would combine a photodetector based on SWNT and a scintillator. The first step of sensor fabrication was to separate HiPco SWNTs dissolved in SDS solution by their chirality. The separated SWNTs were used as ingredients to fabricate the photodetector. The photodetector based on the separated carbon nanotube worked in the whole range of the wavelength. When the light was on, the voltage occurred. However, the detector showed brilliant efficiency in the range of the near IR by the original properties of carbon nanotube. When the detector is exposed to radiation, the combination of a detector based on SWNTs and a scintillator which emits long wavelength (NIR) is expected to make a good radiation detector. However, when the photodetector with the scintillator that emission wavelength was not fit to SWNT or was weak such as BGO (Bismuth germanium oxide), detector based SWNTs cannot work effectively enough as a radiation detector. Therefore, the ultimate goal of this research is to fabricate an effective radiation detector based on SWNT which would be combined with a photodetector based on the separated SWNT and a scintillator which emits suitable wavelength for the separated SWNT.

Reference

[1] S. Iijima, "Helical microtubules of graphitic carbon," Nature 354, 56–58. (1991)

[2] Z. Han, "Thermal conductivity of carbon nanotubes and their polymer nanocomposites: A review," Progress in Polymer Science 36, 914-944. (2011)

[3] H. Liu, D. Nishide, T. Taanaka and H. Kataura, "Large- Scale Single-Chirality Separation of Single-Wall Carbon Nanotubes by Simple Gel Chromatography," Nature Communications, 305, 1-7. (2011)

[4] Y. Shi, L. Ren, and D.Li, "Optimization Conditions for Single-Walled Carbon nanotube Dispersion," Journal of Surface Engineered Materials and Advanced Technology, 3, 6-12. (2013)

[5] R. Sadri et al., "An experimental study on thermal conductivity and viscosity of nanofluids containing carbon nanotubes," Nanoscale Research Letters, 9, 151. (2014)

[6] H. Dai, "Carbon Nanotubes: Synthesis, Integration, and Properties," Accounts of Chemical Research, 35, 1035-1044. (2002)

[7] L. Wei et al., "Formation of single-walled carbon nanotube thin films enriched with semiconducting nanotubes and their application in photoelectrochemical devices," Nanoscale, 3, 1845-1849. (2011)

[8] Z. Wu, Z. Chen et al., "Transparent, Conductive Carbon Nanotube Films," Science, 305, 5688. (2004)

[9] F. Wang, K. Matsuda et al. "Considerably improved photovoltaic performance of carbon nanotube-based solar cells using metal oxide layers," Nature Communications, 6:6305. (2015)

[10] P. Ghai et al. "Carbon Nanotubes in Photovoltaics," International Advanced Research Journal in Science, 2, 1. (2015)

[11] C. D. Cress et al. "Radiation effects in single-walled carbon nanotube papers," Journal of Applied Physics, 107, 014316. (2010)

[12] C. D. Cress et al. "Radiation Effects in Carbon Nanoelectronics," Electronics 1, 23-31. (2012)

[13] M. J. O'Connell, R. E. Smalley et al. "Band Gap Fluorescence from Indiviual Single-Walled Carbon Nanotubes," Science, 297, 593-596, (2002)

[14] Pierson HO, "Handbook of carbon, graphite, diamond and fullerenes: properties," Processing and applications, New Jersey: Noyes Publications (1993)

[15] Wypych G, "Handbook of fillers: physical properties of fillers and filled materials," Toronto: ChemTec Publishing, (2000)

[16] Fischer JE, "Carbon nanotubes: structure and properties. In: Gogotsi Y, editor," Carbon nanomaterials, 51–8. (2006)

[17] S. Wolff, M. J. Wang, "Carbon black science & technology," 2nd ed. New York: Marcel Dekker. (1993)

[18] Kelly BT, "Physics of graphite," Barking (UK): Applied Science Publishers. (1981)

[19] N. Akchurin, R. Wigmans et al., "A comparison of BGO and BSO crystals used in the dual-readout mode," Nuclear Instruments and Methods in Physics Research, A 640, 91-98. (2011)

[20] W. W. Moses et al., "Prospects of Dense, Infrared, Dnitting Scintillators," IEEE Transactions on Nuclear Science, 45, 462-466 (1998)

[21] C.A Cooper, R. J. Young, M. Halsall, "Investigation into the deformation of carbon nanotubes and their composites through the use of Raman spectroscopy," Composites Part A: Applied Science and Manufacturing, 32, 401-411. (2001)

[22] G. Gao, T. Cagin, W. A. Goddard, "Energetics sturucture, mechanical and vibrational properties of single-walled carbon nanotubes," Nanotechnology, 9, 184. (1998)

[23] K. Awasthi, A. Srivastava, O. N. Srivastava, "Synthesis of carbon nanotubes,", Journal of nanoscience and nanotechnology 5, 1616-1636. (2005)

[24] T. Spires, R. M. Brown, "High Resolution TEM Observations of Single-Walled Carbon Nanotubes," Department of Botany, The University of Texas at Austin, Austin, Tx., 78713, (1996)

[25] P. M. Ajayan, "Nanotubes from Carbon", Chemical Reviews, 99, 1787-1799 (1999).

[26] E. T. Thostenson, Z. Ren, T. Chou, "Advances in the science and technology of carbon nanotubes and their composites: a review," Composites science and technology, 61, 1899-1912. (2001)

[27] D. O. Kim, J. Nam, "Polymeric Carbon Nanotube Nanocomposites," Prospectives of Industrial Chemistry," 9, 3-13. (2006)

[28] 5.R. Saito, G. Dresselhaus, and M. S. Dresselhaus, "Physical Properties of Carbon Nanotubes," Imperial College, London, (1998).

[29] J. U. Lee, "Photovoltaic effect in ideal carbon nanotube diodes," Applied Physics Letters, 87,

073101 (2005)

[30] A. A. Kamminskii, “Crystalline Lasers: Physical Processes and Operating Schemes,” Boca Raton: CRC Press, Inc. (1996)

[31] L.Xun, “Fabrication of CsI(Tl) microcolumnar structure scintillator by glancing angle deposition (GLAD),” Chonnam National University. (2013)

[32] A. Lekawa-Raus, J. Patmore, K. Kozil et al.. “Electrical Properties of Carbon Nanotube Based Fibers and Their Future Use in Electrical Wiring,” Advanced Functional Materials, 24, 3661-3682. (2014)

[33] Q. Li, Y. Li, X. Zhang, S. B. Chikkannanavar, W. Zhao, A. M. Dangelewicz, L. Zheng, S. K. Doorn, Q. Jia, D. E. Peterson, P. N. Arendt, and Y. Zhu, “Structure-Dependent Electrical Properties of Carbon Nanotube Fibers,” Advanced Materials, 19, 3358-3363. (2007)

[34] M. B. Jakubinek, J. B. Johnson, M. A. White, C. Jayasinghe, G. Li, W. D. Cho, M. J. Schulz, V. Shanov, “Thermal and electrical conductivity of array-spun from different carbon nanotube yarns,” Carbon, 50, 244-248 (2012)

[35] H. W. Zhu, C. L. Xu, D. H. Wu, B. Q. Wei, R. Vajtai, P. M. Ajayan, “Direct Synthesis of Long Single-Walled Carbon Nanotube Strands,” Science, 296, 884-886. (2002)

[36] W. Zhou, J. Vavro, K. Guthy, K. I. Winey, J. E. Fischer, L. M. Ericson, S. Ramesh, R. Saini, V. A. Davis, C. Kittrell, M. Pasquali, R. H. Hauge, R. E. Smalley, “Single Wall Carbon Nanotube Fibers Extruded from Super-Acid Suspensions: Preferred Orientation, Electrical and Thermal Transport,” Journal of Applied Physics, 95, 649-655 (2004)

[37] N. Behabtu, C. C. Young, D. E. Tsentalovich, O. Kleinerman, X. Wang, A. W. K. Ma, E. A. Bengio, R. F. ter Waarbeek, J. J. de Jong, R. E. Hoogerwerf, S. B. Fairchild, J. B. Ferguson, B. Maruyama, J. Kono, Y. Talmon, Y. Cohen, M. J. Otto, M. Pasquali, “Strong, Light, Multifunctional Fibers of Carbon Nanotubes with Ultrahigh Conductivity,” Science, 339, 182-186. (2013)

[38] J. N. Barisci, M. Tahhan, G. G. Wallace, S. Badaire, T. Vaugien, M. Maugey, P. Poulin, “Properties of Carbon Nanotube Fibers Spun from DNA-Stabilized Dispersions,” Advanced Functional Materials, 14, 133-138. (2004)

[39] X.-H. Zhong, Y.-L. Li, Y.-K. Liu, X.-H. Qiao, Y. Feng, J. Liang, J. Jin, L. Zhu, F. Hou, J.-Y. Li, “Continuous Multilayered Carbon Nanotube Yarns,” Advanced Materials, 22, 692-696. (2010)

[40] L. Song, G. Toth, J. Wei, Z. Liu, W. Gao, L. Ci, R. Vajtai, M. Endo, P. M. Ajayan, “Sharp burnout

failure observed in high current-carrying double-walled carbon nanotube fibers," Nanotechnology, 23, 015703. (2012)

[41] P. R. Bandaru, "Electrical Properties and Applications of Carbon Nanotube Structures," Journal of Nanoscience and Nanotechnology, 7, 1-29 (2007)

Acknowledgements

Thank you for professor Chang Young Lee, adviser, and members in Carbon Nanomaterial Lab. I was a first student of prof. Lee's laboratory, and I was immature. During I was belonging the lab, I had a chance to improve. I always enjoyed in the lab, and with laboratory members and professor. The time I spent in the lab was a treasure for me.